International Journal of Nanomedicine

Dovepress
open access to scientific and medical research

Open Access Full Text Article

ORIGINAL RESEARCH

Nanosilver/poly (DL-lactic-co-glycolic acid) on titanium implant surfaces for the enhancement of antibacterial properties and osteoinductivity

This article was published in the following Dove Medical Press journal:
International Journal of Nanomedicine

Xuemin Zeng,[1,2] Shijiang Xiong,[1,3] Shaoyang Zhuo,[1,4] Chunpeng Liu,[1,2] Jie Miao,[5] Dongxu Liu,[1,2] Hengxiao Wang,[6] Yueying Zhang,[6] Zhong Zheng,[7,8] Kang Ting,[8] Chunling Wang,[1,2] Yi Liu[1,2]

[1]Shandong Provincial Key Laboratory of Oral Tissue Regeneration, School of Stomatology, Shandong University, Jinan, People's Republic of China; [2]Department of Orthodontics, School of Stomatology, Shandong University, Jinan, People's Republic of China; [3]Department of Endodontics, School of Stomatology, Shandong University, Jinan, People's Republic of China; [4]Department of Oral Maxillofacial Surgery, School of Stomatology, Shandong University, Jinan, People's Republic of China; [5]Department of Stomatology, The 5th People's Hospital of Jinan, Jinan, People's Republic of China; [6]Department of Experimental Pathology, Institute of Basic Medicine, Shandong Academy of Medical Sciences, Jinan, People's Republic of China; [7]Section of Orthodontics, Division of Growth and Development, School of Dentistry, University of California, Los Angeles, CA, USA; [8]UCLA Division of Plastic and Reconstructive Surgery, Department of Orthopaedic Surgery, Orthopaedic Hospital Research Center, University of California, Los Angeles, CA, USA

Background: Despite titanium (Ti) implants have been commonly used in the medical device field due to their superior biocompatibility, implant-associated bacterial infection remains a major clinical complication. Nanosilver, an effective antibacterial agent against a wide spectrum of bacterial strains, with a low-resistance potential, has attracted much interest too. Incorporation of nanosilver on Ti implants may be a promising approach to prevent biofilm formation.

Purpose: The objective of the study was to investigate the antibacterial effects and osteoinductive properties of nanosilver/poly (DL-lactic-co-glycolic acid)-coated titanium (NSPTi).

Methods: Gram-positive methicillin-resistant *Staphylococcus aureus* (MRSA) and the Gram-negative opportunistic pathogen *Pseudomonas aeruginosa* (PAO-1) were used to evaluate the antibacterial activity of NSPTi implants through the analysis of bacterial colonization in vitro and in vivo. Furthermore, we examined the osteoinductive potential of NSPTi implants by investigating the proliferation and differentiation of MC3T3-E1 preosteoblast cells. In vivo, the osteoinductive properties of NSPTi implants were assessed by radiographic evaluation, H&E staining, and Masson's trichrome staining.

Results: In vitro, bacterial adhesion to the 2% NSPTi was significantly inhibited and <1% of adhered bacteria survived after 24 hours. In vitro, the average colony-forming units (CFU)/g ratios in the 2% NSPTi with 10^3 CFU MRSA and PAO-1 were 1.50±0.68 and 1.75±0.6, respectively. In the uncoated Ti groups, the ratios were $1.03\pm0.82\times10^3$ and $0.94\pm0.49\times10^3$, respectively. These results demonstrated that NSPTi implants had prominent antibacterial properties. Proliferation of MC3T3-E1 cells on the 2% NSPTi sample was 1.51, 1.78, and 2.22 times that on the uncoated Ti control after 3, 5, and 7 days' incubation, respectively. Furthermore, NSPTi implants promoted the maturation and differentiation of MC3T3-E1 cells. In vivo, NSPTi accelerated the formation of new bone while suppressing bacterial survival.

Conclusion: NSPTi implants have simultaneous antibacterial and osteoinductive activities and therefore have the potential in clinical applications.

Keywords: silver nanoparticles, Ti, antimicrobial, osteogenesis, infection

Introduction

It is a challenging task to treat implant-associated bacterial infections that are severe complications in orthopedics. Implant-associated bacterial infections can lead to increased patient morbidity and may consequently lead to worse results.[1–5] Management of an implant-associated infection often necessitates multiple debridement surgeries, implant replacement or removal, and long-term antibiotic treatment.[6–9] These problems are aggravated in patients with bone healing disorders associated with rheumatoid arthritis, osteoporosis, diabetes, or aging due to the difficulty of clearing an infection

Correspondence: Yi Liu; Chunling Wang
Shandong Provincial Key Laboratory of Oral Tissue Regeneration, School of Stomatology, Shandong University, No.44-1 Wenhuaxi Road, Jinan, 250012, People's Republic of China
Tel +86 531 8838 2070
Fax +86 531 8838 2923
Email yiliu@sdu.edu.cn; wangchl@sdu.edu.cn

submit your manuscript | www.dovepress.com
Dovepress
http://dx.doi.org/10.2147/IJN.S190954

from poorly vascularized bone tissues and other necrotic tissues.[3,5,10,11] Implant-associated infections are caused by bacterial adhesion to an implant surface and subsequent formation of biofilms around implanted devices.[12] After implantation, a rapid conditioning layer covers the surface of the implant and facilitates bacterial adhesion, forming a slimy extracellular polymeric substance (EPS) bacterial biofilm.[5,12,13] The EPS blocks the penetration of antibiotics and host immune cells, because the altered chemical microenvironment in the biofilm associated with nutrient and oxygen consumption causes some bacteria more resistant to antimicrobial and immune cells killing.[5,14–16] Consequently, once a bacterial biofilm is produced, treating the infections is quite difficult, and bacteria in EPS biofilm form can be less susceptible to antibiotics or immune-reactive molecules than free-floating bacteria.[17] Multiple approaches have attempted to prevent infection and bacterial biofilm formation, in particular, surface coating strategies using antibacterial or antiadhesive materials that inhibit microbial infection while simultaneously promoting bone formation seems to be promising.

Although current antibiotics have been coated on orthopedic material surface to prevent infection, binding specificity of a designated bacteria to a specific conventional antimicrobial limits the clinical utility of local antibiotics.[18–21] Because a wide variety of bacterial species are responsible for implant-associated infections: Gram-positive *Staphylococcus* bacteria species (*Staphylococcus aureus*, *Staphylococcus epidermidis*, *Staphylococcus hominis*, and *Staphylococcus haemolyticus*) and Gram-negative *Pseudomonas aeruginosa* and *Escherichia coli*, among which, *S. aureus* and *P. aeruginosa* are the two most common pathogens for implant infection.[22–24] Narrow-spectrum antibiotic therapies may fail to prevent all implant-associated infecting bacteria, while broad-spectrum antibiotic therapies may induce antibiotic resistance. Treatment of infections becomes even more difficult due to the emergence of increasing number of antibacterial resistant bacteria, such as vancomycin-resistant *S. aureus* (VRSA) and methicillin-resistant *S. aureus* (MRSA).[24]

Silver, an antimicrobial agent against a wide spectrum of Gram-positive and Gram-negative bacterial strains including MRSA, VRSA, and methicillin-resistant *S. epidermidis*, has been widely employed to treat infections.[18,25,26] It has been speculated that several mechanisms are associated with the antibacterial performance of silver such as structural damage to bacterial function, inhibition of bacterial function, and induction of bacterial apoptosis-like response;[28,29] and the multilevel antimicrobial mode ensures that bacterial resistance cannot be easily acquired. Furthermore, previous studies have suggested that silver antimicrobial actions affect at least three bacterial cell systems, and silver resistance needs to have three high frequency distinct mutations, so silver-resistant bacteria are not common in clinical cases.[30–32]

Due to their extremely large surface area and surface reactivity, compared with traditional silver counterparts, nanosilver particles exhibit superior physicochemical and biomedical properties, including antimicrobial activity and catalysis.[33] The United States Food and Drug Administration (FDA)-approved, biocompatible and biodegradable polymer poly (DL-lactic-co-glycolic acid) (PLGA) was chosen in this research to stabilize nanosilver particles mainly because of its autocatalytic hydrolysis reaction through nucleophilic interactions with nanoparticles.[34] In the present work, the antibacterial effects and osteoinductive properties of nanosilver/PLGA-coated titanium (NSPTi) implants were investigated through in vitro and in vivo studies in rabbits.

Materials and methods

Pretreatment of Ti samples

Titanium, of 99.5% purity, was purchased from BaoTi Group Co., Ltd. (Xian, People's Republic of China). Initial, Ti bars (Φ 1×10 mm) and discs (thickness: 1.0 mm, diameter: 6.5 mm) were mechanically wet abraded with abrasive SiC papers (1,200 grit). In order to improve surface roughness and remove native oxide, the Ti samples were etched using a mixed acid solution (H_2SO_4:HCl:H_2O =2:2:1, volume ratio) at 50°C for 4 hours. Then, the samples were soaked in NaOH solution (100 mL of 5 M NaOH) at 60°C for 4 hours to increase surface hydrophilicity. After ultrasonic cleaning and air drying, the samples were sterilized by ultraviolet irradiation for 30 minutes.

Preparation of nanosilver/PLGA coatings

Nanosilver/PLGA coatings were obtained by solvent casting, mixing 20–30 nm diameter spherical nanosilver (Shanghai Naiou Nanotechnology Co., Ltd, Shanghai, People's Republic of China) with 18% (w/v) PLGA (Daigang Biomaterial Co., Ltd, Jinan, People's Republic of China, lactic:glycolic ratio =85:15, inherent viscosity: 0.64 dL/g in chloroform; Sigma-Aldrich Co., St Louis, MO, USA) solution at 300 rpm for 1 hour thoroughly. Coatings were produced by adding Ag nanoparticles at 1 and 2 wt% (designated as 1% NSPTi and 2% NSPTi, respectively) with respect to PLGA. Ti bars and discs were immersed in the nanosilver/PLGA solution in chloroform at room temperature for 45 seconds and thoroughly air-dried. The immersion and dry processes were

repeated three times to ensure a homogenized coating for each NSPTi implant sample.

Characterization of coatings

The morphology and composition of the NSPTi implant surface were characterized using field-emission scanning electron microscopy (SEM) (HITACHI SU8010, Tokyo, Japan) equipped with an X-ray energy-dispersive spectrometer (EDS).

Culture of cells and cell viability assessment

MC3T3-E1 mouse preosteoblasts were obtained from Chinese Academy of Sciences Shanghai Cell Bank (Shanghai, People's Republic of China). The cells were seeded on NSPTi discs and incubated at 37°C in a 5% CO_2 environment with 500 mL osteogenic medium (α-Minimum Essential Medium supplied with 10% FBS, 100 nM dexamethasone, 1% penicillin–streptomycin, 50 μg/mL ascorbic acid, and 10 mM β-glycerophosphate). All media for cell culture were purchased from Invitrogen (Carlsbad, CA, USA). Cell counting kit-8 (Dojindo Molecular Technologies, Kumamoto, Japan) was used to identify potential cellular toxicity of the samples. The cell density was 2×10^4 cells/sample.

Ag release

The release of Ag from NSPTi samples (1% NSPTi and 2% NSPTi) in PBS was monitored by inductively coupled plasma–atomic emission spectrometry (Thermo Fisher ICP6300, Waltham, MA, USA) analyzing the resulting set of PBS solutions. The samples were incubated in PBS (6 mL, pH 7.4) at 37°C in dark conditions for 24 hours and rinsed with deionized water. The whole procedure was repeated for up to 14 days. The detection limit of Ag in this method was 0.001 ppm, and the emission line was 328.1 nm.

Antibacterial tests in vitro

The antibacterial properties of the coatings were evaluated against Gram-positive MRSA (ATCC43300; American Type Culture Collection [ATCC], Manassas, VA, USA) and Gram-negative PAO-1 (ATCC15442; ATCC).[22–24] MRSA and PAO-1 were inoculated into Luria–Bertani (LB; Sigma-Aldrich Co.) broth medium. Initially, the uncoated Ti 1% NSPTi and 2% NSPTi were incubated in 10^3 or 10^5 colony-forming units (CFU) bacterial suspensions (in culture broth) with shaking at 200 rpm at 37°C for 1, 2, 6, and 24 hours. Next, adherent bacteria on each sample bar were suspended in sterilized PBS by sonication for 30 seconds at 40 kHz using a sonication device (BactoSonic; BANDELIN GmbH, Berlin, Germany)[35] and plated onto 10 cm LB culture medium plates.[36] After incubation, the colonies were quantitated by aerobic plate count method according to procedures described in the FDA Bacteriological Analytical Manual (BAM). Concisely, the whole bacteria collected in 1 mL sterilized PBS was inoculated into plates and diluted if number of CFU per plate exceeded 250. If number of CFU per plate was in the range of 25–250, total number of colonies counted was recorded. If number of CFU per plate was >250, the bacterial solution was diluted (1:10, 1:100, and 1:1,000) until the resulting number of CFU was within 25–250 per plate range, and number of colonies was then calculated.

Osteoinductivity in vitro

ALP activity (normalized to the total protein concentration) and degree of mineralization were employed to determine the osteoinductive potential of NSPTi implants on osteoblastic differentiation. ALP is an early phenotypic marker for osteogenic differentiation, and the formation of mineralized nodules caused by the calcium secretion of MC3T3-E1 cells is an important functional indicator of osteoblasts.[37,38] The ALP activity was standardized to the total cellular protein concentration, which was determined with a BCA protein assay kit (Tiangen Biotech Company, Beijing, People's Republic of China). ALP activity was detected by an ALP assay kit (Jiancheng Biotech, Nanjing, People's Republic of China). The extent of matrix mineralization was determined by Alizarin red staining (Sigma-Aldrich Co.).

Animals and surgical procedures

Sixteen adult male New Zealand White rabbits, average weight 3 kg, were used in the full study. All surgical procedures were approved and performed according to the guidelines of the Institutional Animal Care and Use Committee of Shandong University. After shaving and disinfection operations, the rabbits were anesthetized by an intraperitoneal injection with 2% pentobarbital sodium (30 mg/kg; Sigma-Aldrich Co.). Local anesthesia was induced with 1 mL of 2% lidocaine (Sigma-Aldrich Co.) to control bleeding. Five intramedullary cavities were drilled on each tibia of rabbits, followed by implantation of sample bars (uncoated Ti and 2% NSPTi). Subsequently, MRSA or PAO-1 suspended in 100 μL sterile PBS (10^4 CFU/mL) was slowly injected into the tibia canal using a micropipette. The micropipette was left for 30 seconds in place to prevent the suspension of the bacteria from leaking out along the injection track. Then, the micropipette was removed. At the end of the procedure, the fascia and skin were closed

with 4–0 Vicryl absorbable sutures (Vicryl Rapide, Ethicon, Johnson & Johnson, Livingston, UK). Operated rabbits were housed separately and fed a commercial pelleted diet. Operated rabbits were monitored daily. Analgesics were injected intramuscularly for 3 days to control pain, and no antibiotics were administered.

Clinical evaluation

A digital thermometer (OMRON, Dalian, People's Republic of China) was used to measure body temperature. Fresh venous blood was obtained for the assessment of white blood cells (WBCs). Clinical signs and symptoms of infection (healing of incisions, appearance of the soft tissues, diarrhea, and lameness) following surgery were monitored. Clinical information was collected on days 0, 3, and 8 and weeks 2, 4, 6, and 8 postsurgery.

Radiographic evaluation

At 2, 4, 6, and 8 weeks after surgery, the operated rabbit tibias were scanned using cone beam computed tomography CBCT (NewTom 5 G, QR Verona, Verona, Italy) while the animals were under general anesthesia. Radiographs were taken at a peak tube voltage of 110 kV, a tube current of 4.2–4.6 mA, and an exposure time of 5.4 seconds. A reconstruction volume of 15×15 cm and a voxel size of 0.3 mm were used. Three-dimensional reconstruction was performed using the threshold and region growing technique with Mimics software, version 17.0 (Materialise, Leuven, Belgium). The animals were sacrificed 8 weeks postoperatively through air embolism. Operated tibias were dissected and harvested for microbiological and histological assessment.

Microbiological evaluation in vivo

Tibia bone tissue samples were split, cut into little pieces, frozen in liquid nitrogen, and crushed in an autopulverizer. The pulverized bone (500 mg) was suspended in 6 mL of PBS and centrifuged for 30 seconds at 10,000 rpm. Serial dilutions were made and plated onto the plates and incubated at 37°C for 24 hours. After incubation, the number of colonies per plate was counted for each tibia bone samples and the bacterial count was calculated per gram bone (CFU/g bone tissue).

Histological evaluation

Tibia bone tissue samples were fixed for 48 hours in 4% formaldehyde/PBS (pH 7.4), decalcified in 10% EDTA in PBS (0.5 M) for 3–4 weeks, dehydrated in ethanol, cleared with xylene, embedded in paraffin, and routinely processed for histological evaluation. Tissue sections of 5 μm were cut and stained with H&E and Masson's trichrome collagen in order to evaluate morphology and inflammation.

Statistical analysis

Data are depicted as mean ± standard error of mean. Statistical analyses were performed using SPSS 16.0 software (SPSS Inc., Chicago, IL, USA). Independent sample *t*-test and one-way ANOVA were used to detect statistically significant differences. Statistical significance was set at $P<0.05$.

Results

Characterization of NSPTi implants

NSPTi implants were obtained by repeated incubations of titanium in nanosilver/PLGA-chloroform solution. A uniform layer (46.23±0.06 μm thickness as shown in Figures 1A, B, and 2A) of nanosilver/PLGA coating was formed on the surface of the titanium implant samples. SEM showed that deposition or clusters of silver nanoparticles were not observed in the coating to contain up to 2 wt% (2% NSPTi) (Figures 1A, B, and S1). EDS line scan was performed across the nanosilver/PLGA coatings to determine the element distribution in the coatings (Figure 2A). The elemental analysis by EDS indicated the presence of Ag within the nanosilver/PLGA coatings (Figure 2B), and the

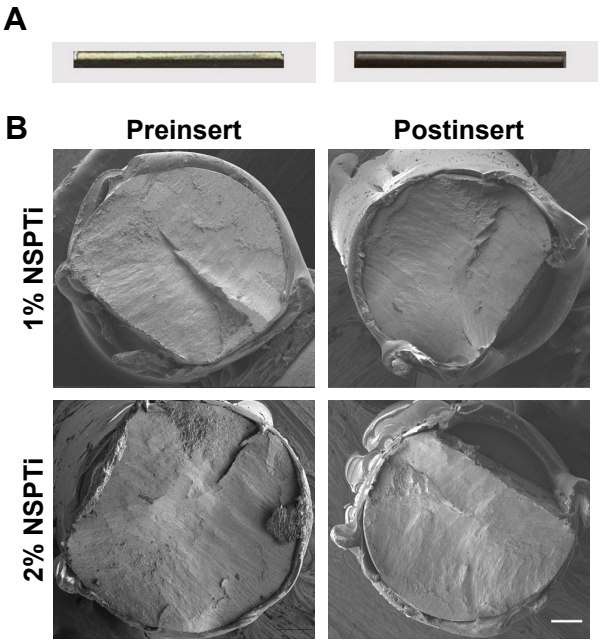

Figure 1 (**A**) Light microscope images of NSPTi samples. (**B**) SEM images of NSPTi samples (preinsert and postinsert).
Notes: A uniform layer of silver nanoparticle/PLGA coating was observed on the surface of the titanium sample. The thickness of the nanosilver/PLGA coating was 46.23±0.06 μm. Placing NSPTi samples into the prereamed intramedullary canal did not considerably damage the coating. White scale bar =100 μm.
Abbreviations: NSPTi, nanosilver/poly (DL-lactic-co-glycolic acid)-coated titanium; PLGA, poly (DL-lactic-co-glycolic acid); SEM, scanning electron microscopy.

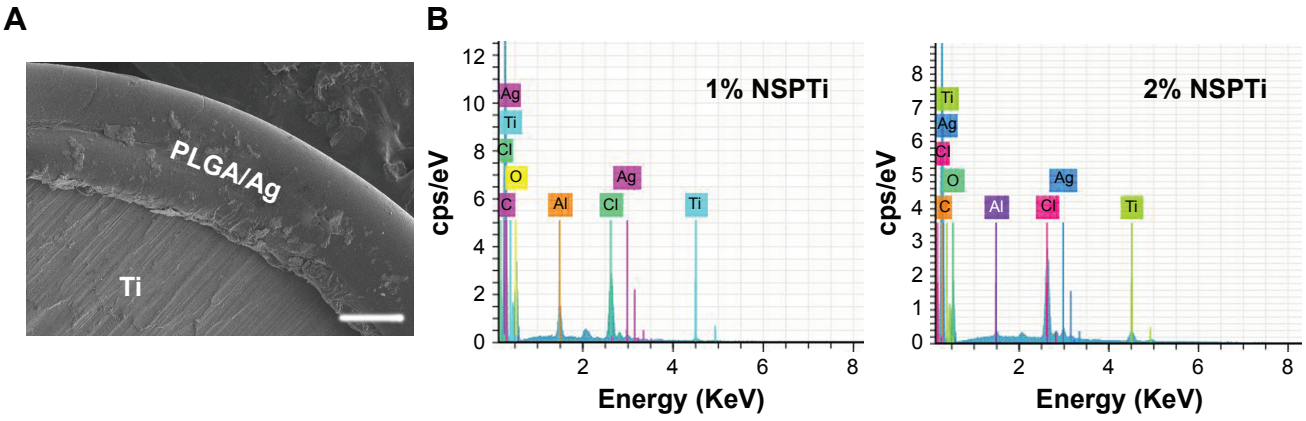

Figure 2 EDS scanning along the cross-section of nanosilver/PLGA coating (**A**). Elements in nanosilver/PLGA coatings detected by EDS (**B**). White scale bar =20 μm.
Abbreviations: EDS, energy-dispersive spectroscopy; NSPTi, nanosilver/poly (DL-lactic-co-glycolic acid)-coated titanium; PLGA, poly (DL-lactic-co-glycolic acid).

content of Ag in the coating is 0.95 and 1.93 wt% for the 1% NSPTi and 2% NSPTi coatings, respectively (Table 1).

Ag release kinetics

Ag release from the NSPTi samples (1% NSPTi and 2% NSPTi) was monitored once the samples were exposed to PBS (pH 7.4). Figure 3 shows the amount of detected Ag in the resulting PBS solutions, where the NSPTi samples were incubated in darkness. For two NSPTi sample groups, the concentration of released Ag followed the same pattern, although the absolute value is dependent on the Ag inside the nanosilver/PLGA coatings. Specifically, the release was significant at the initial 4 days of incubation. The rate of release started to decrease after day 4 and it became negligible after day 10 (Figure 3). The maximum amount of released Ag was 0.067 and 0.117 ppm for the 1% NSPTi and 2% NSPTi samples, respectively, at day 1. At the plateau stage after 10 days, the amount of released Ag was 0.014 ppm per day. After 14 days' incubation, ~82% (1.66 mg) and 73% (2.964 mg) silver released from the 1% NSPTi and 2% NSPTi samples, respectively.

Antibacterial tests in vitro

Antibacterial experiments in vitro indicated that the uncoated Ti control did not inhibit bacterial adhesion or proliferation, while nanosilver-concentration-dependent bactericidal behavior was observed in the NSPTi samples (1% NSPTi and 2% NSPTi). When uncoated titanium was incubated with 10^3 CFU of either MRSA or PAO-1, ~98% of the bacteria initially adhered to the sample in 1 hour, and bacteria proliferated significantly with time (Figure 4A and C). The initial adhesion of 10^3 CFU MRSA or PAO-1 to 2% NSPTi samples was <10% (Figure 4A and C); after 24 hours of incubation, only limited bacterial colonies were observed (Figure 4A and C). The 1% NSPTi implant group slightly reduced the initial adhesion of 10^3 CFU MRSA or PAO-1 and significantly inhibited their proliferation. When the initial inoculum of both species was 10^5 CFU, ~2×10^3 bacteria initially adhered to the uncoated Ti control samples and proliferated with incubation time (Figure 4B and D). In the 2% NSPTi group incubated with 10^5 CFU MRSA or PAO-1, the bacteria initially adhered to the samples was ~1.6×10^3, and their proliferation decreased markedly (Figure 4B and D). In contrast, initial bacterial adhesion to

Table 1 Composition of nanosilver/PLGA coatings, as determined using EDS

Sample	Mass %					
	C	O	Cl	Ti	Al	Ag
1% NSPTi	65.61	28.14	3.73	0.41	1.16	0.95
2% NSPTi	69.07	22.43	4.86	1.45	0.26	1.93

Note: The weight percentage of Ag is 0.95 and 1.93 for the 1% NSPTi and 2% NSPTi coatings, respectively.
Abbreviations: EDS, energy-dispersive spectroscopy; NSPTi, nanosilver/poly (DL-lactic-co-glycolic acid)-coated titanium; PLGA, poly (DL-lactic-co-glycolic acid).

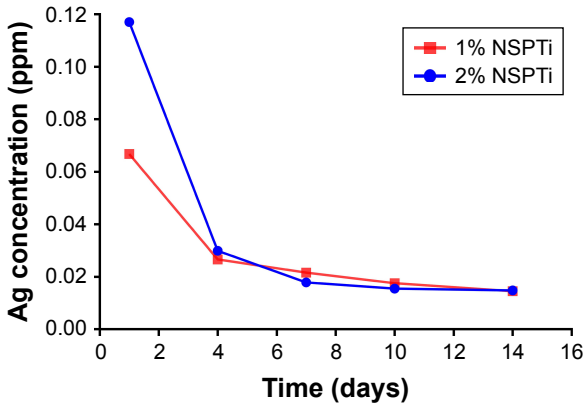

Figure 3 Noncumulative silver release profiles from NSPTi samples (1% NSPTi and 2% NSPTi) into PBS.
Abbreviation: NSPTi, nanosilver/poly (DL-lactic-co-glycolic acid)-coated titanium.

the 2% NSPTi samples was significantly inhibited and <1% of adhered bacteria survived after 24 hours, although the initial inoculum of MRSA or PAO-1 was increased to 10^5 CFU (Figure 4B and D).

Osteogenic activity of NSPTi implants in vitro

CCK-8 assay was carried out to compare MC3T3-E1 cell proliferation on the uncoated Ti and NSPTi samples

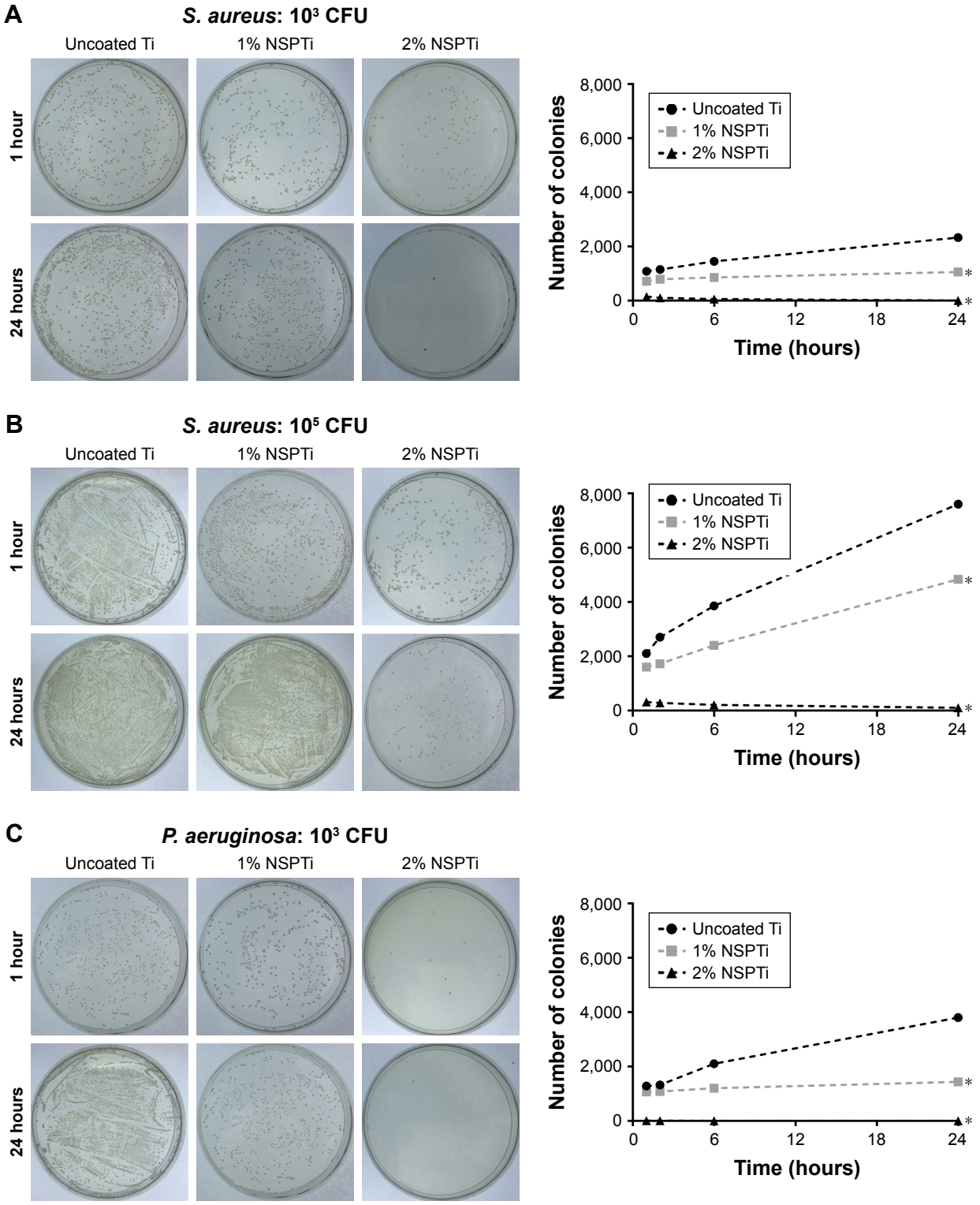

Figure 4 (*Continued*)

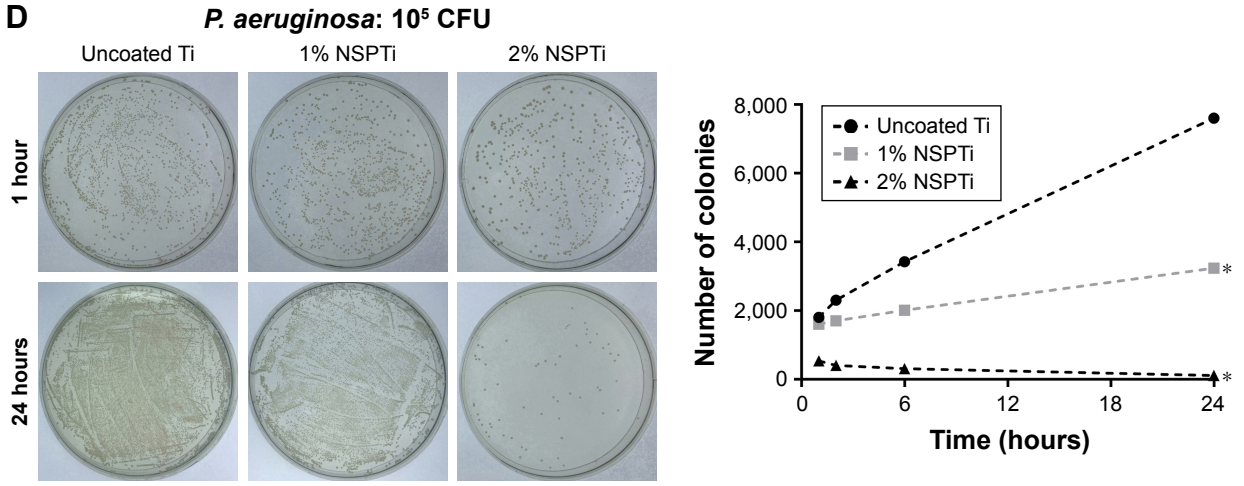

Figure 4 In vitro bacterial colonization analysis of MRSA (**A** and **B**) and PAO-1 (**C** and **D**).
Notes: The antimicrobial activity of uncoated Ti and NSPTi samples against 10^3 and 10^5 CFU bacterial strains was evaluated. N=6, and * indicates a significant difference compared with uncoated Ti ($P<0.05$). Error bars were too small to show.
Abbreviations: CFU, colony-forming units; MRSA, methicillin-resistant *Staphylococcus aureus*; NSPTi, nanosilver/poly (DL-lactic-co-glycolic acid)-coated titanium; PAO, *Pseudomonas aeruginosa*; *S. aureus*, *Staphylococcus aureus*; Ti, titanium.

quantitatively, which suggested that cellular toxicity was not a concern (Figure 5A). Briefly, MC3T3-E1 cell proliferation in NSPTi groups increased with increasing nanosilver concentrations (Figure 5A). Up to 2% silver particles in NSPTi samples (2% NSPTi) did not reduce MC3T3-E1 cell growth but improved cell proliferation. In addition, NSPTi samples with higher nanosilver concentrations promoted cell proliferation more effectively (Figure 5A). As shown in Figure 5A, proliferation of MC3T3-E1 cells on the 2% NSPTi sample was 1.51, 1.78, and 2.22 times that on the uncoated Ti control after 3, 5, and 7 days of incubation in osteogenic medium, respectively. To investigate the NSPTi effect on osteoblastic differentiation, the ALP activity of MC3T3-E1 cells was quantified after 7 and 14 days as shown in Figure 5B. The ALP activity of MC3T3-E1 cells in each group on day 14 increased dramatically compared with that on day 7. Compared with the uncoated Ti control, NSPTi samples with higher nanosilver concentrations promoted the ALP activity of cell more effectively. As shown in Figure 5C, after 15 and 21 days culture in osteogenic medium, there was obviously more matrix mineralization on the NSPTi samples than on the uncoated Ti control, suggesting that NSPTi samples also significantly increased the terminal differentiation of MC3T3-E1 cells. On day 21, the matrix mineralization of cells on the 2% NSPTi sample was 2.15 times greater than that on the uncoated Ti control (Figure 5C).

Clinical evaluation

Three rabbits in uncoated Ti groups died on days 2 and 8 because of diarrhea and infection, respectively. Four rabbits in the uncoated Ti group showed infection at the surgical site, and there was no significant infection in animals in the 2% NSPTi group. The body temperature in all groups increased significantly during the initial 3 days, then started to decrease gradually from days 3 to 14, and remained relatively constant until day 56. On day 3, the body temperature in the 2% NSPTi group was lower than that in the uncoated Ti group, while there was no notable difference between the uncoated Ti and NSPTi groups from then until day 56 (Figure 6A and C). The WBC count of rabbits in the uncoated Ti group grew gradually during the initial 3 days, but the levels subsequently dropped from days 8 to 56. By contrast, in the 2% NSPTi group, the WBC count increased gradually in the first 8 days, followed by a sustainable decline from days 8 to 56 (Figure 6B and D). Generally, on days 3, 28, 42, and 56, the WBC count in the 2% NSPTi group was less than that in the uncoated Ti group ($P<0.05$).

Radiographic and CT analysis

Eight weeks after implantation, radiographic analysis revealed little bone formation in the tibial canals injected with bacteria in the uncoated Ti group. In addition, there was a significant bone destruction in the tibial canals of rabbits in the infected uncoated Ti group (Figure 7A and B). In contrast, no signs of osteolysis were observed in the infected 2% NSPTi group. Three-dimensional CT reconstruction images showed newly formed bone in the tibial canals of rabbits surrounding the 2% NSPTi implants (Figure 7A and B). Videos S1–S4 confirmed these results.

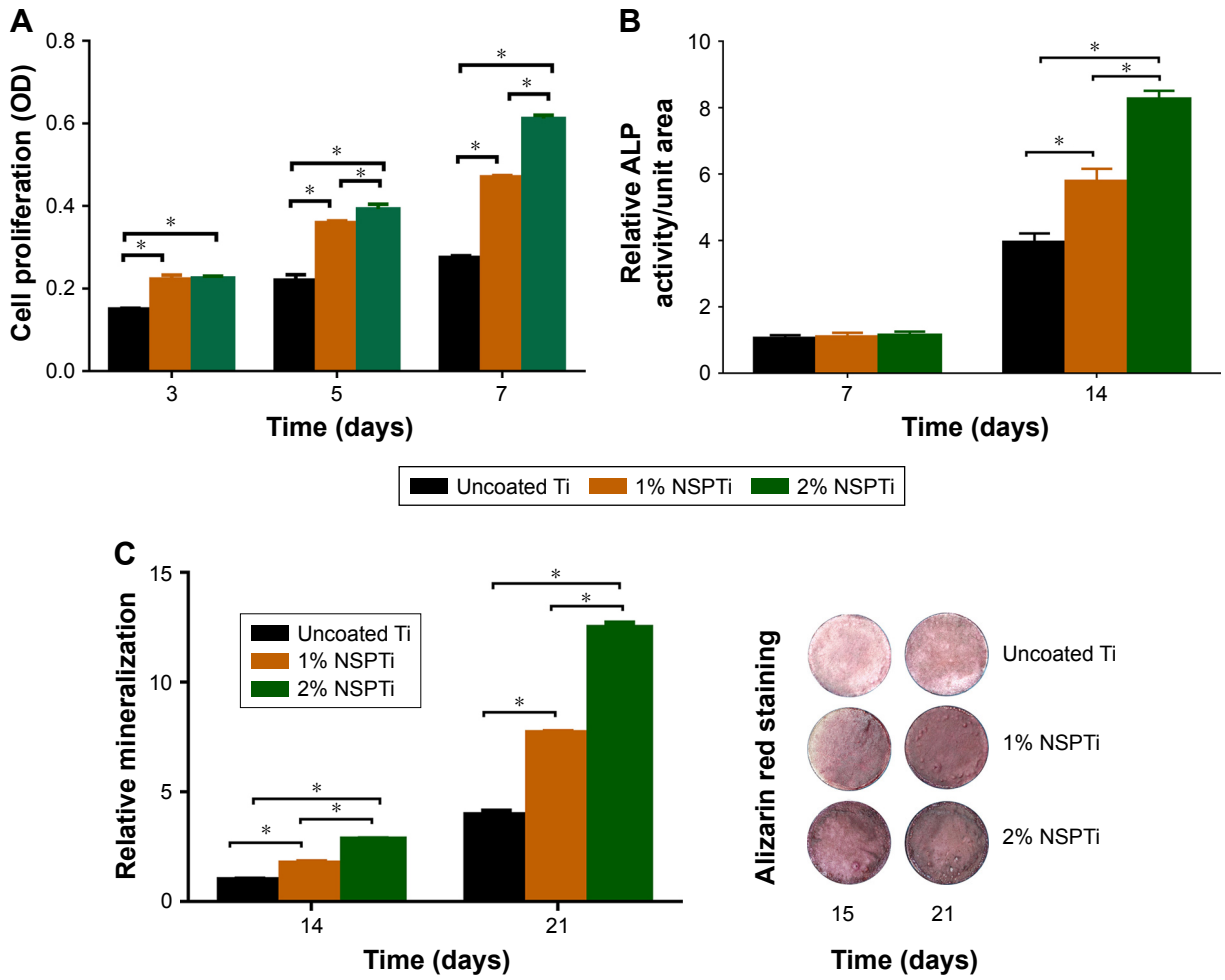

Figure 5 In vitro osteoinductive activity of NSPTi.
Notes: NSPTi significantly promoted MC3T3-E1 cell proliferation (**A**), ALP activity (**B**), and mineralization (**C**). Data were normalized to the uncoated Ti control on day 7 (**B**) and on day 14 (**C**). N=6, *$P<0.05$.
Abbreviations: N, number; NSPTi, nanosilver/poly (DL-lactic-co-glycolic acid)-coated titanium; OD, optical density; Ti, titanium.

Microbiological evaluation in vivo

The average CFU/g ratios in the 2% NSPTi group injected with 10^3 CFU MRSA and PAO-1 were 1.50±0.68 and 1.75±0.6, respectively. In the uncoated Ti group, the ratios were $1.03±0.82×10^3$ and $0.94±0.49×10^3$, respectively. Bacterial colonization in the 2% NSPTi group was significantly less than that in the uncoated Ti group ($P<0.05$; Figure 8).

Histological results

Histological sections of tibia bone samples were subjected to H&E and Masson's trichrome staining to visualize and assess the new bone formation. Eight weeks after implantation, signs of inflammation (Figure 9B) were evident around uncoated Ti implants in the tibial canals with 10^3 CFU MRSA or PAO-1. No apparent evidence of bone formation was present around the uncoated Ti implants in the infected tibial canals of rabbits (Figure 9A, C, and D), and the result was in accordance with radiographic analysis. In contrast, significant newly formed bone appeared around 2% NSPTi implants under the same processing conditions 8 weeks after implantation (Figure 9A, C, and D). Moreover, minimal inflammatory cell infiltration was detected around 2% NSPTi implants, which indicated that 2% NSPTi implants significantly prevented bacterial colonization and did not induce obvious inflammatory responses in vivo. No significant nanosilver toxicity was found in the 2% NSPTi group. Taken together, 2% NSPTi implants exhibited significant antibacterial properties and osteoinductivity in vivo due to the presence of nanosilver in a concentration-dependent manner.

Discussion

Ag-based compounds and Ag ions are antimicrobial agents against a wide spectrum of bacterial strains, with a low-resistance potential, and hence have been widely employed

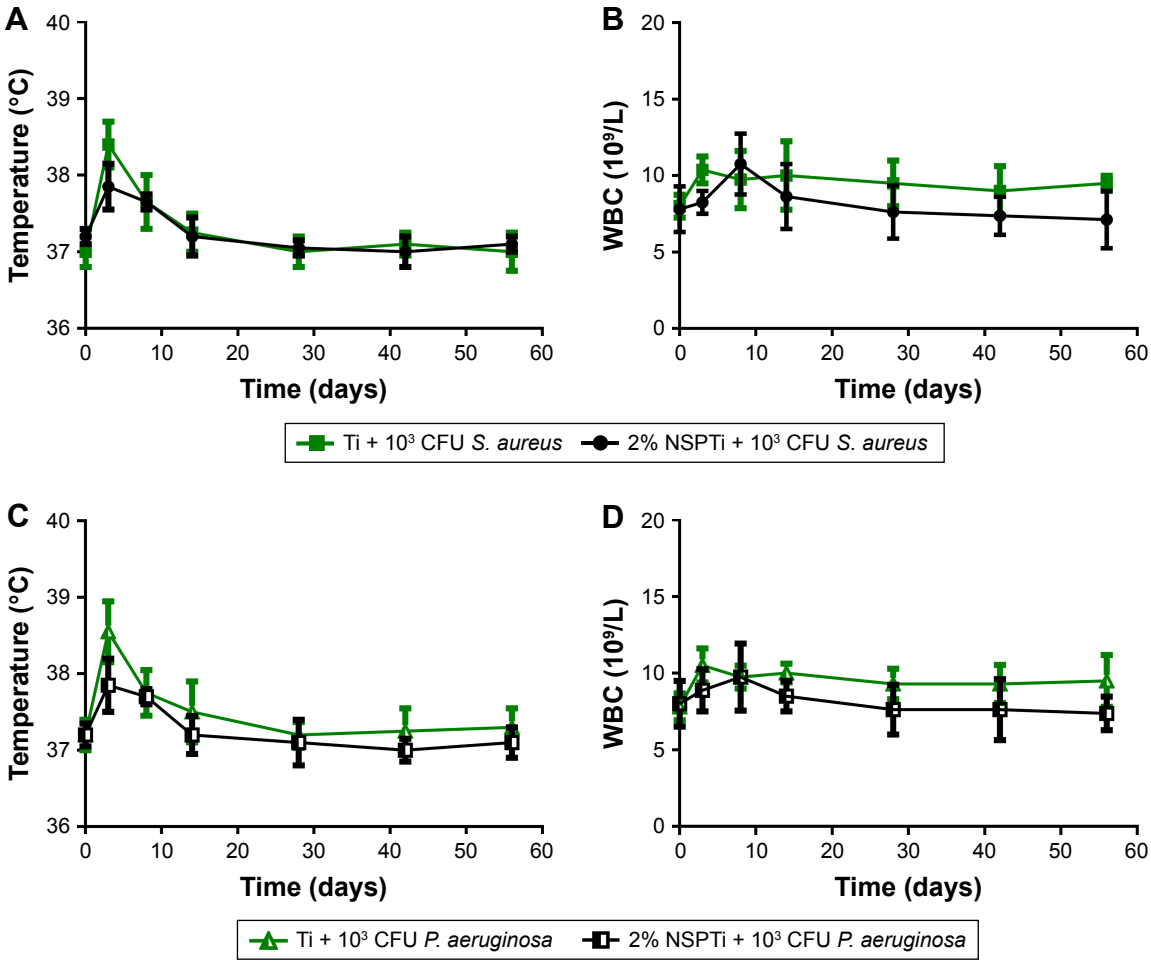

Figure 6 Change patterns of the body temperature (**A** and **C**) and WBC (**B** and **D**) in rabbits from day 0 to day 56. MRSA or PAO-1 in 100 μL sterile PBS (10^5 CFU) was injected into the tibial canals of rabbits after implantation for bacterial invasion. N=8.

Abbreviations: CFU, colony-forming units; MRSA, methicillin-resistant *Staphylococcus aureus*; N, number; NSPTi, nanosilver/poly (DL-lactic-co-glycolic acid)-coated titanium; PAO, *Pseudomonas aeruginosa*; *S. aureus*, *Staphylococcus aureus*; Ti, titanium; WBC, white blood cell.

to treat infections in medical field.[28] Nanosilver particles are small in size, have a huge surface-to-volume ratio, possess unique physicochemical properties, and have no charge compared with conventional non-nanoscale silver.[34] It has been speculated that several mechanisms are involved in the antibacterial performance of nanosilver. Nanosilver particles inhibit bacterial cell division, leading to cell death by destructing bacterial membrane structures.[29] They also cause a bacterial apoptosis-like response by inducing the generation of reactive oxygen species, which can lead to impaired physiological function through oxidative damage to cell macromolecules.[31] Most importantly, nanosilver particles are known to elicit antimicrobial properties due to their large surface-to-weight ratio, which in turn provides a larger area for microbial contact. Researches indicated that 5–50 nm silver nanosilver particles have antimicrobial properties against microorganisms[32] and that 10–30 nm nanosilver particles effectively suppress pathogens and show no statistically cytotoxicity.[39] In this study, 20–30 nm diameter spherical nanosilver particles were utilized.

Several polymers have been used to stabilize nanosilver particles because of their tendency to agglomerate and form large clusters, including polyallylamine,[40] polyethylenimine,[41] chitosan,[42] and poly (vinyl-pyrrolidone).[43] By donating electrons, the polymers can bind together with metal particles due to their superior nucleophilic properties.[44]

The FDA-approved, biocompatible and biodegradable polymer PLGA was chosen for the present research as a delivery system due to its hydrolysable ester bonds, which were subjected to nucleophilic interactions with nanosilver particles.[35] PLGA degradation is involved in hydrolytic chain scission and transport of products, which are normal metabolic pathways in the body.

Due to the excellent biocompatibility, nanosilver/PLGA coating do not require surgical removal and could display antibacterial activity without evoking a host

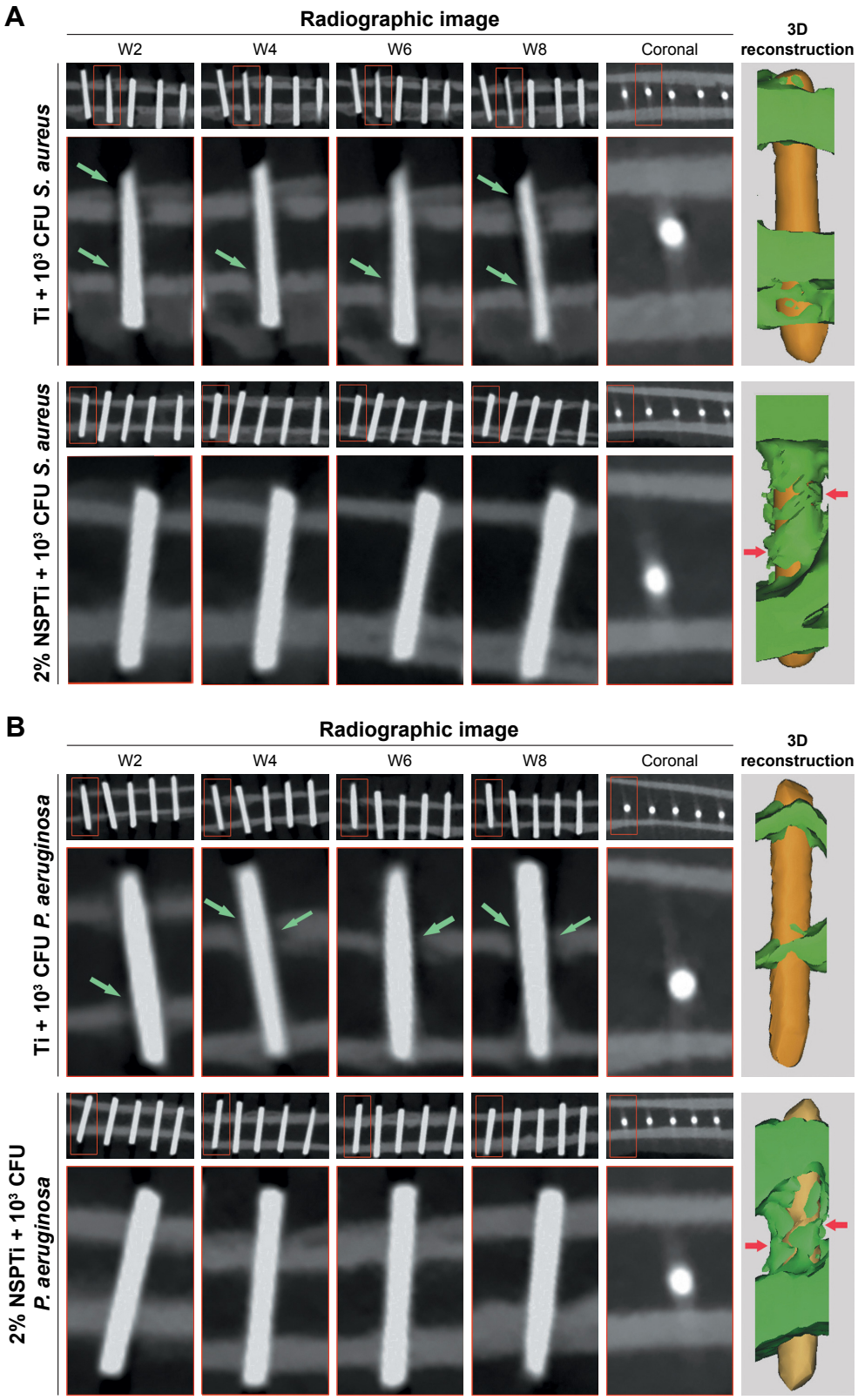

Figure 7 Radiographic images and reconstruction images of infected Ti (**A**) and 2%-NSPTi implants (**B**) in the tibial canals of rabbits.

Notes: MRSA or PAO-1 in 100 μL sterile PBS (10^4 CFU/mL) was injected into the tibial canals after implantation. There was significant bone destruction (green arrows) in the tibial canals of rabbits in the infected uncoated Ti group. No obvious radiographic signs of bone formation were observed in the infected uncoated Ti group up to 8 weeks postsurgery, while in the infected 2% NSPTi group, significant bone formation surrounding 2% NSPTi implants was observed (red arrows). In addition, no bone destruction was observed in the infected 2% NSPTi group.

Abbreviations: CFU, colony-forming units; MRSA, methicillin-resistant *Staphylococcus aureus*; NSPTi, nanosilver/poly (DL-lactic-co-glycolic acid)-coated titanium; PAO, *Pseudomonas aeruginosa*; *S. aureus*, *Staphylococcus aureus*; Ti, titanium.

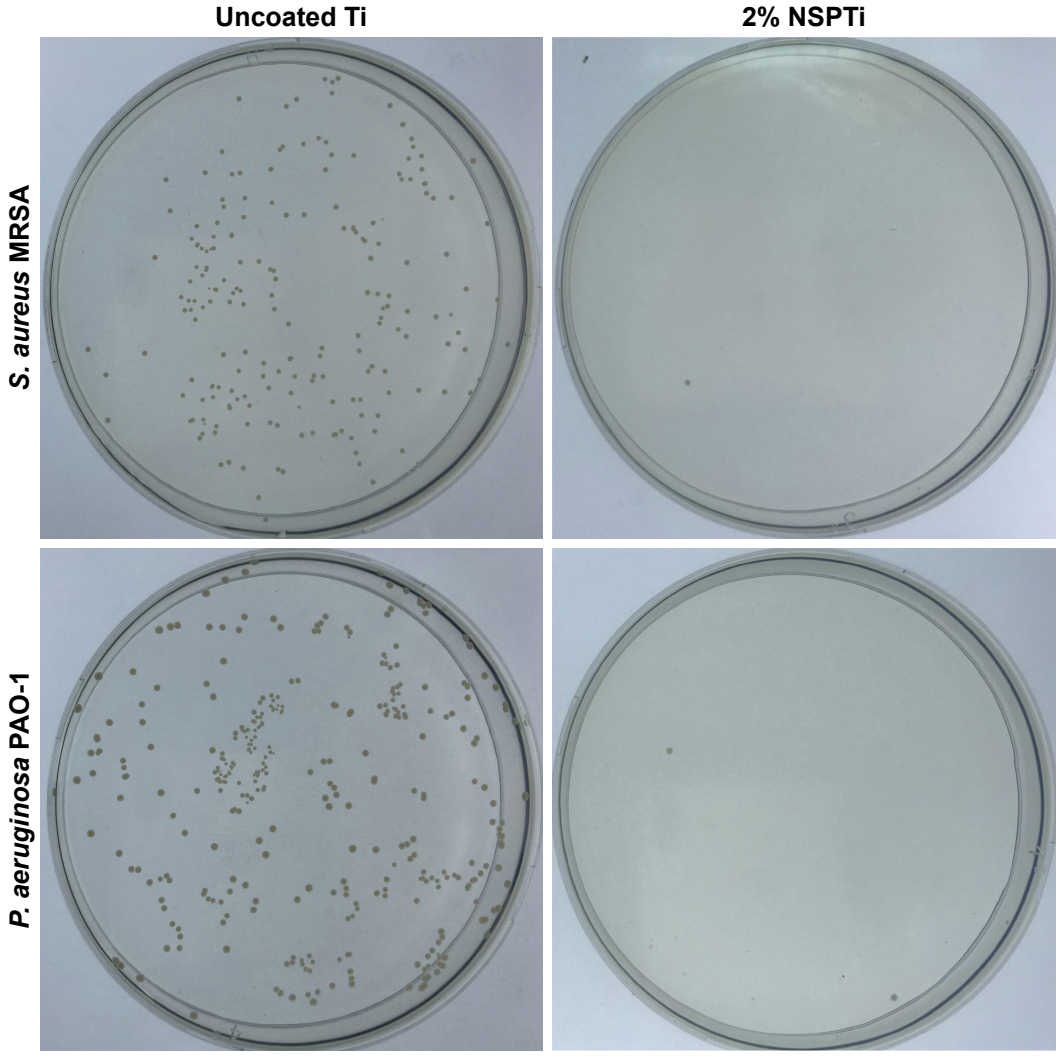

Figure 8 Bacterial colony formation of tibial bone tissues.
Note: Bacterial colonization in the 2% NSPTi group was significantly lower than those in uncoated Ti group.
Abbreviations: MRSA, methicillin-resistant *Staphylococcus aureus*; NSPTi, nanosilver/poly (DL-lactic-co-glycolic acid)-coated titanium; PAO, *Pseudomonas aeruginosa*; *S. aureus*, *Staphylococcus aureus*; Ti, titanium.

immune response. The uniform distribution of nanosilver particles in nanosilver/PLGA coating was facilitated by using the PLGA polymer matrix as a stabilizing system for nanosilver silver. The SEM images show no aggregates of silver nanoparticles in the coatings consisting of up to 2% silver nanoparticles (Figures 1A, B, and S1). In our study, the 2% nanosilver/PLGA coating demonstrated no toxicity to cells (Figure 5A). PLGA, as polymer matrix, can slow down and sustain the release kinetics of bactericides (Ag) in nanosilver/PLGA coating, since high doses of Ag could be detrimental to biocompatibility. The nanosilver/PLGA coating could provide a satisfactory antibacterial protection on Ti implant surface against bacterial infections (Figure 3). The release of silver was significant at the initial 4 days, followed by active release from days 4 to 10, and then the plateau was observed, which depicts a low but sustained release (Figure 3). Experiments in in vitro indicated that 2% NSPTi implants significantly inhibited bacterial colonization and bacterial biofilm formation after invasive orthopedic and dental surgery (Figure 4A and B). For the in vivo studies in the tibial canals of rabbits, 2% NSPTi implants displayed significant antibacterial activity against 10^3 CFU MRSA or PAO-1 (Figures 7A, B, and 9), which are typical bacteria responsible for invasive tissue infection.[22–24] Osteogenic potency has long been highly desirable for the orthopedic and dental implants. Therefore, we tried to assess the osteoinductive properties of NSPTi implants. Interestingly, the results from the ALP and Alizarin red staining assays showed that 2% NSPTi coatings significantly improved cell proliferation and differentiation (Figure 5A–C). Significant newly formed bone appeared around 2% NSPTi implants in infected rabbit (Figures 7A, B and 9A, C, D). The findings

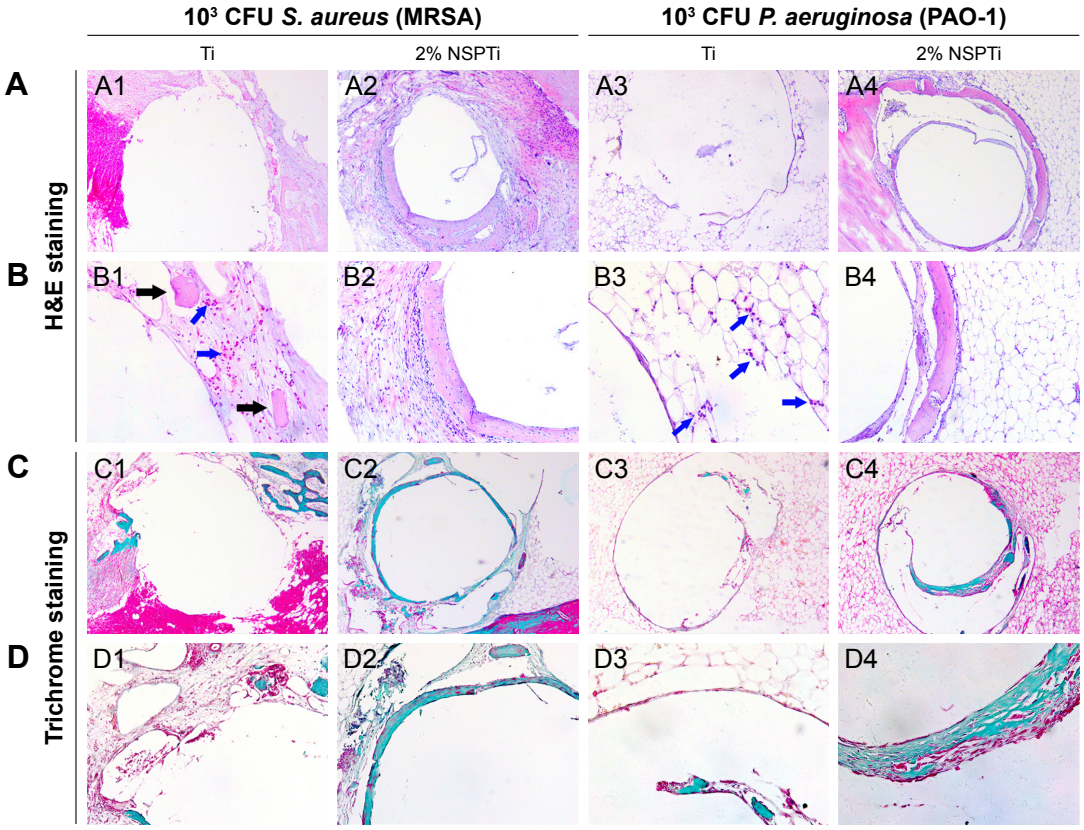

Figure 9 Histological analysis of Ti and 2% NSPTi implants in tibial bone tissues at 8 weeks after implantation; 10^3 CFU MRSA or PAO-1 in 100 μL sterile PBS (10^4 CFU/mL) was injected into the canal before implantation.

Notes: H&E staining (**A** and **B**) suggested acute or chronic presence of inflammatory cells (blue arrows) with intramedullary abscesses and necrotic disintegrating bone fragments (black arrows) in the intramedullary tissue around uncoated Ti implants, while 2% NSPTi implants showed no apparent signs of bone infection. Consistent with the radiographic analysis, there was little bone formation around uncoated Ti implants, whereas significant bone formation (red arrows) was observed around 2% NSPTi implants, as shown by H&E staining (**A** and **B**) and Masson's trichrome staining (**C** and **D**). **A** and **B** were to visualize and assess the new bone formation (A1–A4) and inflammation (B1–B4). **C** (C1–C4) and **D** (D1–D4) were used to evaluate new bone collagen. For **A**, magnification =50×. For B1 and B3, magnification =200×. For B2 and B4, magnification =100×. Column **D** is magnification of column **C**. For **C**, magnification =50×. For **D**, magnification =100×.

Abbreviations: MRSA, methicillin-resistant *Staphylococcus aureus*; NSPTi, nanosilver/poly (DL-lactic-co-glycolic acid)-coated titanium; PAO, *Pseudomonas aeruginosa*; *S. aureus*, *Staphylococcus aureus;* Ti, titanium.

indicate that NSPTi implants significantly inhibit bacterial colonization and bacterial biofilm formation due to the presence of silver. Additionally, 2% NSPTi implants markedly improved bone formation although incubated with an initial bacterial inoculum. The osteoinductive properties of NSPTi implants can be explained by the fact that nanosilver inhibits cell division through disrupting multiple components of bacterial structure, function, and metabolism and induces specific effects of cell macromolecules (DNA, protein, lipid, and others) through oxidative damage.[27,28]

Conclusion

In this study, NSPTi implants exhibited superior antibacterial and osteoinductive activity compared with uncoated titanium implants, which make NSPTi implants promising candidates for applications in orthopedic surgery. The concentration of nanosilver in the coating can be higher in further research. Elucidating the mechanism of osteoinductive activity of NSPTi implants is essential in further research.

Acknowledgments

This study was supported by the National Natural Science Fund of China (81701008), the Natural Science Foundation of Shandong Province (BS2015YY027, ZR2018LH012), the China Postdoctoral Science Foundation (2014M561941), Special Funds for Postdoctoral Innovation Projects of Shandong Province (201402030), and the Fundamental Research Funds of Shandong University (2016GN009). No benefits in any form have been received or will be received from any commercial party related directly or indirectly to the subject of this article.

Disclosure

The authors report no conflicts of interest in this work.

References

1. Bakhshandeh S, Gorgin Karaji Z, Lietaert K, et al. Simultaneous delivery of multiple antibacterial agents from additively manufactured porous biomaterials to fully eradicate planktonic and adherent *Staphylococcus aureus*. *ACS Appl Mater Interfaces*. 2017;9(31):25691–25699.

2. Muller AE, Punt N, Mouton JW. Optimal exposures of ceftazidime predict the probability of microbiological and clinical outcome in the treatment of nosocomial pneumonia. *J Antimicrob Chemother*. 2013;68(4):900–906.
3. Giavaresi G, Borsari V, Fini M, et al. Preliminary investigations on a new gentamicin and vancomycin-coated PMMA nail for the treatment of bone and intramedullary infections: an experimental study in the rabbit. *J Orthop Res*. 2008;26(6):785–792.
4. Croes M, Bakhshandeh S, van Hengel IAJ, et al. Antibacterial and immunogenic behavior of silver coatings on additively manufactured porous titanium. *Acta Biomater*. 2018;81:315–327.
5. Darouiche RO. Treatment of infections associated with surgical implants. *N Engl J Med*. 2004;350(14):1422–1499.
6. Tan Y, Leonhard M, Moser D, Ma S, Schneider-Stickler B. Long-term antibiofilm activity of carboxymethyl chitosan on mixed biofilm on silicone. *Laryngoscope*. 2016;126(12):E404–E408.
7. Hegde V, Dworsky EM, Stavrakis AI, et al. Single-dose, preoperative vitamin-D supplementation decreases infection in a mouse model of periprosthetic joint infection. *J Bone Joint Surg Am*. 2017;99(20):1737–1744.
8. Riool M, de Breij A, Drijfhout JW, Nibbering PH, Zaat SAJ. Antimicrobial peptides in biomedical device manufacturing. *Front Chem*. 2017;5:63.
9. Uppuluri P, Busscher HJ, Chakladar J, van der Mei HC, Chaffin WL. Transcriptional profiling of *C. albicans* in a two species biofilm with *Rothia dentocariosa*. *Front Cell Infect Microbiol*. 2017;7:311.
10. Stewart PS, William Costerton J. Antibiotic resistance of bacteria in biofilms. *Lancet*. 2001;358(9276):135–138.
11. Donlan RM. Biofilms: microbial life on surfaces. *Emerg Infect Dis*. 2002;8(9):881–890.
12. Zilberman M, Elsner JJ. Antibiotic-eluting medical devices for various applications. *J Control Release*. 2008;130(3):202–215.
13. Truong VK, Pham VT, Medvedev A, et al. Self-organised nanoarchitecture of titanium surfaces influences the attachment of *Staphylococcus aureus* and *Pseudomonas aeruginosa* bacteria. *Appl Microbiol Biotechnol*. 2015;99(16):6831–6840.
14. Batoni G, Maisetta G, Esin S. Antimicrobial peptides and their interaction with biofilms of medically relevant bacteria. *Biochim Biophys Acta*. 2016;1858(5):1044–1060.
15. Kargupta R, Bok S, Darr CM, et al. Coatings and surface modifications imparting antimicrobial activity to orthopedic implants. *Wiley Interdiscip Rev Nanomed Nanobiotechnol*. 2014;6(5):475–495.
16. Esposito S, Leone S. Prosthetic joint infections: microbiology, diagnosis, management and prevention. *Int J Antimicrob Agents*. 2008;32(4):287–293.
17. Rabin N, Zheng Y, Opoku-Temeng C, du Y, Bonsu E, Sintim HO. Biofilm formation mechanisms and targets for developing antibiofilm agents. *Future Med Chem*. 2015;7(4):493–512.
18. Darouiche RO. Antimicrobial approaches for preventing infections associated with surgical implants. *Clin Infect Dis*. 2003;36(10):1284–1289.
19. Li H, Bidzilya OV. Review of the genus *Gnorimoschema* Busck, 1900 (Lepidoptera, Gelechiidae) in China. *Zootaxa*. 2017;4365(2):173–195.
20. Nie B, Long T, Ao H, Zhou J, Tang T, Yue B. Covalent immobilization of enoxacin onto titanium implant surfaces for inhibiting multiple bacterial species infection and in vivo methicillin-resistant *Staphylococcus aureus* infection prophylaxis. *Antimicrob Agents Chemother*. 2016;61(1):e01766-16.
21. Antoci V, King SB, Jose B, et al. Vancomycin covalently bonded to titanium alloy prevents bacterial colonization. *J Orthop Res*. 2007;25(7):858–866.
22. Chen R, Willcox MD, Ho KK, Smyth D, Kumar N. Antimicrobial peptide melimine coating for titanium and its in vivo antibacterial activity in rodent subcutaneous infection models. *Biomaterials*. 2016;85:142–151.
23. Atefyekta S, Ercan B, Karlsson J, et al. Antimicrobial performance of mesoporous titania thin films: role of pore size, hydrophobicity, and antibiotic release. *Int J Nanomedicine*. 2016;11:977–990.
24. Campoccia D, Montanaro L, Arciola CR. The significance of infection related to orthopedic devices and issues of antibiotic resistance. *Biomaterials*. 2006;27(11):2331–2339.
25. Nanda A, Saravanan M. Biosynthesis of silver nanoparticles from *Staphylococcus aureus* and its antimicrobial activity against MRSA and MRSE. *Nanomedicine*. 2009;5(4):452–456.
26. Mekkawy AI, El-Mokhtar MA, Nafady NA, et al. In vitro and in vivo evaluation of biologically synthesized silver nanoparticles for topical applications: effect of surface coating and loading into hydrogels. *Int J Nanomedicine*. 2017;12:759–777.
27. Eckhardt S, Brunetto PS, Gagnon J, Priebe M, Giese B, Fromm KM. Nanobio silver: its interactions with peptides and bacteria, and its uses in medicine. *Chem Rev*. 2013;113(7):4708–4754.
28. Tian X, Jiang X, Welch C, et al. Bactericidal effects of silver nanoparticles on lactobacilli and the underlying mechanism. *ACS Appl Mater Interfaces*. 2018;10(10):8443–8450.
29. Bondarenko OM, Sihtmäe M, Kuzmičiova J, Ragelienė L, Kahru A, Daugelavičius R. Plasma membrane is the target of rapid antibacterial action of silver nanoparticles in *Escherichia coli* and *Pseudomonas aeruginosa*. *Int J Nanomedicine*. 2018;13:6779–6790.
30. Silver S, Phung Let, Silver G. Silver as biocides in burn and wound dressings and bacterial resistance to silver compounds. *J Ind Microbiol Biotechnol*. 2006;33(7):627–634.
31. Leaper DJ. Silver dressings: their role in wound management. *Int Wound J*. 2006;3(4):282–294.
32. Woodmansey EJ, Roberts CD. Appropriate use of dressings containing nanocrystalline silver to support antimicrobial stewardship in wounds. *Int Wound J*. 2018;15(6):1025–1032.
33. Shevlin D, O'Brien N, Cummins E. Silver engineered nanoparticles in freshwater systems – likely fate and behaviour through natural attenuation processes. *Sci Total Environ*. 2018;621:1033–1046.
34. Houchin ML, Topp EM. Chemical degradation of peptides and proteins in PLGA: a review of reactions and mechanisms. *J Pharm Sci*. 2008;97(7):2395–2404.
35. Thomaidis PC, Pantazatou A, Kamariotis S, et al. Sonication assisted microbiological diagnosis of implant-related infection caused by *Prevotella disiens* and *Staphylococcus epidermidis* in a patient with cranioplasty. *BMC Res Notes*. 2015;8(1):307.
36. Liu D, He C, Liu Z, Xu W. Gentamicin coating of nanotubular anodized titanium implant reduces implant-related osteomyelitis and enhances bone biocompatibility in rabbits. *Int J Nanomedicine*. 2017;12:5461–5471.
37. Wang G, Zheng L, Zhao H, et al. In vitro assessment of the differentiation potential of bone marrow-derived mesenchymal stem cells on genipin-chitosan conjugation scaffold with surface hydroxyapatite nanostructure for bone tissue engineering. *Tissue Eng Part A*. 2011;17(9–10):1341–1349.
38. Sehgal RR, Carvalho E, Banerjee R, Stiff M. Mechanically stiff, zinc cross-linked nanocomposite scaffolds with improved osteostimulation and antibacterial properties. *ACS Appl Mater Interfaces*. 2016;8(22):13735–13747.
39. Venugopal A, Muthuchamy N, Tejani H, et al. Incorporation of silver nanoparticles on the surface of orthodontic microimplants to achieve antimicrobial properties. *Korean J Orthod*. 2017;47(1):3–10.
40. Dotzauer DM, Dai J, Sun L, Bruening ML. Catalytic membranes prepared using layer-by-layer adsorption of polyelectrolyte/metal nanoparticle films in porous supports. *Nano Lett*. 2006;6(10):2268–2272.
41. Kuo PL, Chen WF, Huang HY, Chang IC, Dai SA. Stabilizing effect of pseudo-dendritic polyethylenimine on platinum nanoparticles supported on carbon. *J Phys Chem B*. 2006;110(7):3071–3077.
42. Ercan B, Kummer KM, Tarquinio KM, Webster TJ. Decreased Staphylococcus aureus biofilm growth on anodized nanotubular titanium and the effect of electrical stimulation. *Acta Biomater*. 2011;7(7):3003–3012.
43. Travan A, Pelillo C, Donati I, et al. Non-cytotoxic silver nanoparticle-polysaccharide nanocomposites with antimicrobial activity. *Biomacromolecules*. 2009;10(6):1429–1435.
44. Shibata T, Tostmann H, Bunker B, et al. XAFS studies of gold and silver-gold nanoparticles in aqueous solutions. *J Synchrotron Radiat*. 2001;8(Pt 2):545–547.

Supplementary materials

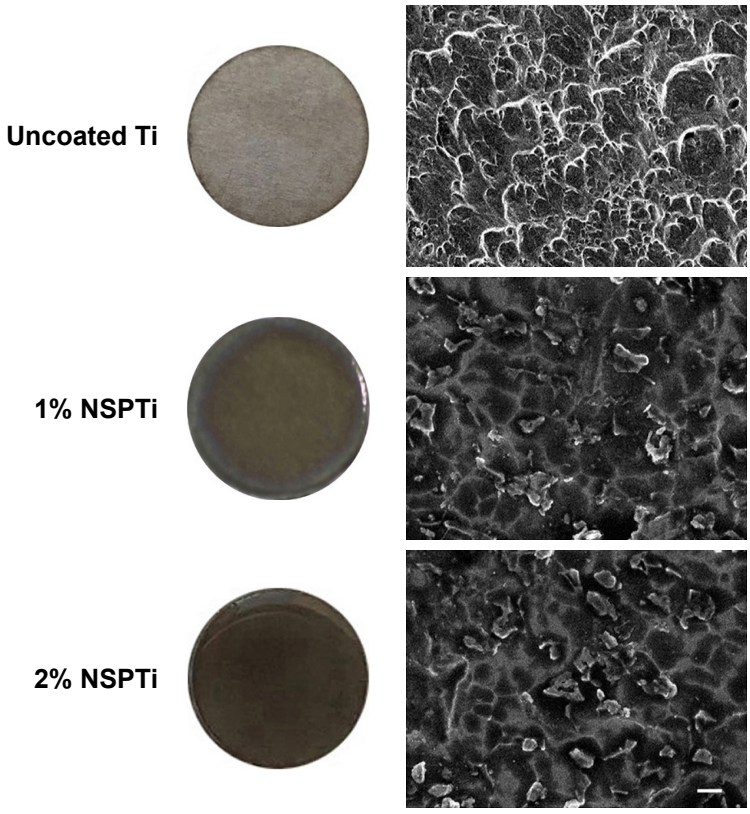

Figure S1 SEM images of uncoated Ti and NSPTi samples.
Notes: There were no silver nanoparticle clusters in the nanosilver/PLGA coatings. White scale bars =5 μm.
Abbreviations: NSPTi, nanosilver/poly (DL-lactic-co-glycolic acid)-coated titanium; PLGA, poly (DL-lactic-co-glycolic acid); SEM, scanning electron microscopy; Ti, titanium.

Videos S1–S4

The supplementary videos include four 3D reconstruction videos of infected titanium and nanosilver/poly (DL-lactic-co-glycolic acid)-coated titanium implants in the rabbits tibial canals. 10^3 colony-forming units methicillin-resistant *Staphylococcus aureus* or *Pseudomonas aeruginosa* in 100 μL sterile PBS (10^4 colony-forming units/mL) was injected into the canal before implantation.

Video S1 3D reconstruction video of Ti implants in the tibial canals with 10^3 CFU MRSA.
Notes: There was no bone formation in the tibial canals of rabbits in the infected uncoated Ti group up to 8 weeks postsurgery (video 1 and video 2), while in the infected 2%-NSPTi group, significant bone formation surrounding 2%-NSPTi implants was observed (Videos S3 and S4).
Abbreviations: CFU, colony-forming units; MRSA, methicillin-resistant *Staphylococcus aureus*; NSPTi, nanosilver/poly (DL-lactic-co-glycolic acid)-coated titanium; Ti, titanium.

Video S2 3D reconstruction video of Ti implants in the tibial canals with 10^3 CFU PAO-1.
Note: There was no bone formation in the tibial canals of rabbits in the infected uncoated Ti group up to 8 weeks postsurgery (Videos S1 and S2), while in the infected 2%-NSPTi group, significant bone formation surrounding 2%-NSPTi implants was observed (Videos S3 and S4).
Abbreviations: CFU, colony-forming units; NSPTi, nanosilver/poly (DL-lactic-co-glycolic acid)-coated titanium; PAO-1, *Pseudomonas aeruginosa*; Ti, titanium.

Video S3 3D reconstruction video of 2%-NSPTi implants in the tibial canals with 10^3 CFU MRSA.
Note: There was no bone formation in the tibial canals of rabbits in the infected uncoated Ti group up to 8 weeks postsurgery (Videos S1 and S2), while in the infected 2%-NSPTi group, significant bone formation surrounding 2%-NSPTi implants was observed (Videos S3 and S4).
Abbreviations: CFU, colony-forming units; MRSA, methicillin-resistant *Staphylococcus aureus*; NSPTi, nanosilver/poly (DL-lactic-co-glycolic acid)-coated titanium; Ti, titanium.

Video S4 3D reconstruction video of 2%-NSPTi implants in the tibial canals with 10^3 CFU PAO-1.
Note: There was no bone formation in the tibial canals of rabbits in the infected uncoated Ti group up to 8 weeks postsurgery (Videos S1 and S2), while in the infected 2%-NSPTi group, significant bone formation surrounding 2%-NSPTi implants was observed (Videos S3 and S4).
Abbreviations: CFU, colony-forming units; NSPTi, nanosilver/poly (DL-lactic-co-glycolic acid)-coated titanium; PAO-1, *Pseudomonas aeruginosa*; Ti, titanium.